Approximating fault detection linear interval observers using λ-order interval predictors

Jordi Meseguer[1], Vicenç Puig[2,*,†] and Teresa Escobet[2,3]

[1]*CETaqua, Water Technology Centre, Ctra. d'Esplugues 75, Cornellà de Llobregat, 08940 Barcelona, Spain*
[2]*Center for Supervision, Safety and Automatic Control (CS2AC), Universitat Politècnica de Catalunya (UPC), Campus de Terrassa, Edifici Gaia, 08222 Terrassa, Spain*
[3]*Department of Minim, Industrial and ICT Engineering Department, Universitat Politècnica de Catalunya (UPC), School of Engineering of Manresa, 08242 Manresa, Spain*

SUMMARY

Interval observers can be described by an autoregressive-moving-average model while λ-order interval predictors by a moving-average model. Because an autoregressive-moving-average (ARMA) model can be approximated by a moving-average model, this allows establishing the equivalence between interval observers and interval predictors. This paper deals with the fault detection application and focuses on the equivalence between the *λ-order interval predictors* and *the interval observers* from the point of view of the fault detection performance. The paper also proves that it is possible to obtain an equivalent $\lambda-$order interval predictor for a given interval observer with the same fault detection properties by the appropriate selection of the $\lambda-$order. A condition for selecting the minimal order that provides the $\lambda-$order interval predictor equivalent to a given interval observer is derived. Moreover, because the wrapping effect could be avoided by tuning properly the interval observer, we can find an equivalent $\lambda-$order interval predictor such that it also avoids the wrapping effect. Finally, an example based on an industrial servo actuator will be used to illustrate the derived results. Copyright © 2016 John Wiley & Sons, Ltd.

Received 15 June 2013; Revised 11 August 2016; Accepted 30 October 2016

KEY WORDS: observers; predictors; fault detection; intervals

1. INTRODUCTION

Model-based fault detection is based on checking the consistency between the analytical relations obtained from the system model and the online measurements obtained from the sensors installed [1]. One of the standard approaches to check such consistency is by means of generating residuals as the difference between measured values of some system variables provided by the sensors and their estimation provided by the analytical relations obtained from the system model. Model-based fault detection can use different types of model representation in order to generate residuals [2–4], as for example, observers or parity approaches. In practice, modeling errors introduce uncertainty in the model interfering with the fault detection process based on residual generation. This fact has motivated to develop robust model-based approaches of fault detection, which are able to handle with existing uncertainty [2]. Those approaches can be classified into groups: active and passive. The active approach aims to generate residuals that maximize the degree of sensitivity to faults while minimizing the degree of sensitivity to uncertainty. On the other hand, the passive robust

*Correspondence to: Vicenç Puig, Center for Supervision, Safety, and Automatic Control (CS2AC) ,Technical University of Catalonia, BarcelonaTECH , Rambla Sant Nebridi, Terrassa 10. 08222, Spain.
†E-mail: vicenc.puig@upc.edu

approach (the one followed in this paper) relies on enhancing the fault detection robustness at the decision-making stage [5] using an adaptive threshold. In case of considering parametric modelling uncertainty, a model whose parameter values are bounded by intervals, known as an *interval model*, is usually considered (see, e.g., [6–8]). Then, adaptive thresholds are typically generated by considering the set of model trajectories that can be obtained by varying the uncertain parameters within their intervals [7].

Standard residual generation methods have been extended to be able to achieve robustness by means of a passive approach using interval models. In this way, interval observers [9–11] or interval parity space (or equations) [6, 12] have already been proposed in literature. In [7] and [13], a comparison between these different interval-based fault detection approaches has been presented concluding that the gain of the interval observer approach plays an important role because it determines the time evolution of the fault residual sensitivity and the associated adaptive threshold derived from the model structured uncertainty. Moreover, as it is also known in the literature [14] in the case of standard observers, an equivalence between observers and parity space (equations) can be proved by selecting the observer gain such that the observer behaves as a *'dead-beat observer'* [15].

The idea of this paper comes from the fact that according to Gertler [3], an observer can be described by an autoregressive-moving-average (ARMA) model, that is, by an IIR filter. On the other hand, a λ-order (or λ-step ahead) predictor (widely used in time series forecasting or in model predictive control, but rarely used in fault detection) can be described by a moving-average (MA) model of order λ, that is, by an FIR filter. It is known from the literature that an IIR filter (i.e., ARMA model) can be approximated by an FIR filter (i.e., MA model) of infinite order. This fact will be used in this paper to approximate a linear interval observers by λ-order interval predictors in the context of fault detection application. The motivation for doing such approximation is justified from the fact that λ-order interval predictors do not need to propagate the state (as interval observers do) to obtain the interval output estimation. Thus, λ-order interval predictors can avoid those problems associated with uncertain state estimation such as the wrapping effect[‡] [16] because, as the *parity space approach*, system inputs and outputs are just needed to compute the output predictions used to generate the residuals [5]. Moreover, λ-order interval predictors can be viewed as a generalization of the *parity space approach* (that leads to a minimum order (step ahead) predictor equivalent to a *'dead-beat observer'*) because it allows to obtain multiple step ahead predictions. This allows to avoid some drawbacks of the parity space approach as the lack of fault indication persistence because of the fault following effect when faults affect to sensors and actuators [13].

The main contribution of this paper is to propose the $\lambda-$order predictor approach as an alternative to interval observers regarding fault detection applications. The paper also proves that it is possible to obtain an equivalent $\lambda-$order interval predictor for a given interval observer with the same fault detection properties (as e.g., fault indication persistence) by the appropriate selection of the $\lambda-$order. A condition for selecting the minimal order that provides the $\lambda-$order interval predictor equivalent to a given interval observer is derived. Moreover, because the wrapping effect could be avoided by tuning properly the interval observer [17], we can find an equivalent $\lambda-$order interval predictor such also avoids the wrapping effect.

To illustrate the performance of the $\lambda-$order interval predictor approach and its comparison with the interval approach observer in fault detection, a known FDI benchmark based on an industrial servo actuator will be used.

[‡] The ***wrapping effect*** is related to the use of a crude approximation of the interval observer solution set and its iteration using one-step ahead recursion of the state-space observer function. Thereby, at each iteration, the true solution set is wrapped into a superset being its overestimation proportional to its radius. Then, a spurious growth of the enclosures can result if the composition of wrapping and mapping is iterated [16].

The structure of the paper remainder is the following: the way to obtain an λ-order predictor equivalent to an interval observer is presented in Section 2. In Section 3, the performance of observers and their equivalent predictors is analyzed when applied to fault detection in order to show their equivalence. Then, in Section 4, an example based on an industrial servo actuator will be used to illustrate the derived results. Finally, the main conclusions are presented in Section 5.

2. λ-ORDER INTERVAL PREDICTORS AND ITS EQUIVALENCE WITH INTERVAL OBSERVERS

2.1. System set-up

Considering that the system to be monitored can be described by a MIMO linear uncertain dynamic model in discrete-time and state-space form, including faults, as follows[§]

$$\begin{aligned} \boldsymbol{x}(k+1) &= \boldsymbol{A}(\tilde{\boldsymbol{\theta}})\boldsymbol{x}(k) + \boldsymbol{B}(\tilde{\boldsymbol{\theta}})\boldsymbol{u}_0(k) + \boldsymbol{F}_a(\tilde{\boldsymbol{\theta}})\boldsymbol{f}_a(k) \\ \boldsymbol{y}(k) &= \boldsymbol{C}(\tilde{\boldsymbol{\theta}})\boldsymbol{x}(k) + \boldsymbol{F}_y(\tilde{\boldsymbol{\theta}})\boldsymbol{f}_y(k) \end{aligned} \tag{1}$$

where $\boldsymbol{y}(k) \in \Re^{ny}$, $\boldsymbol{u}_0(k)$[¶]$\in \Re^{nu}$, $\boldsymbol{x}(k) \in \Re^{nx}$ are the system output, input, and the state-space vectors, respectively; $\boldsymbol{A}(\tilde{\boldsymbol{\theta}}) \in \Re^{nx\times nx}$, $\boldsymbol{B}(\tilde{\boldsymbol{\theta}}) \in \Re^{nx\times nu}$and $\boldsymbol{C}(\tilde{\boldsymbol{\theta}}) \in \Re^{ny\times nx}$ are the state, the input, and the output matrices, respectively; $\tilde{\boldsymbol{\theta}} \in \Re^{n\theta}$ is the system parameter vector that is not known exactly; $\boldsymbol{f}_y(k) \in \Re^{ny}$ and $\boldsymbol{f}_a(k) \in \Re^{nu}$ are faults in the system output sensors and actuators respectively being $\boldsymbol{F}_y(\tilde{\boldsymbol{\theta}})$ and $\boldsymbol{F}_a(\tilde{\boldsymbol{\theta}})$ as their associated matrices.

The system in (1) can be expressed in input-output form using the shift operator q^{-1} and assuming zero initial conditions as follows:

$$\boldsymbol{y}(k) = \boldsymbol{y}_0(k) + \boldsymbol{G}_{fa}(q^{-1}, \tilde{\boldsymbol{\theta}})\boldsymbol{f}_a(k) + \boldsymbol{G}_{fy}(q^{-1}, \tilde{\boldsymbol{\theta}})\boldsymbol{f}_y(k) \tag{2}$$

where

$$\boldsymbol{y}_0(k) = \left(\boldsymbol{C}(\tilde{\boldsymbol{\theta}})(q\boldsymbol{I} - \boldsymbol{A}(\tilde{\boldsymbol{\theta}}))^{-1}\boldsymbol{B}(\tilde{\boldsymbol{\theta}})\right)\boldsymbol{u}_0(k) \tag{3}$$

and $\boldsymbol{G}_{fa}$, $\boldsymbol{G}_{fy}$ are the system transfer functions considering the system faults ($\boldsymbol{f}_a$, $\boldsymbol{f}_y$) and can be expressed as follows:

$$\boldsymbol{G}_{fa}(q^{-1}, \tilde{\boldsymbol{\theta}}) = \boldsymbol{C}(\tilde{\boldsymbol{\theta}})(q\boldsymbol{I} - \boldsymbol{A}(\tilde{\boldsymbol{\theta}}))^{-1}\boldsymbol{F}_a(\tilde{\boldsymbol{\theta}}) \tag{4}$$

$$\boldsymbol{G}_{fy}(q^{-1}, \tilde{\boldsymbol{\theta}}) = \boldsymbol{F}_y(\tilde{\boldsymbol{\theta}}) \tag{5}$$

2.2. Interval observer

The system described by (1) could be monitored using a linear observer with *Luenberger* structure based on an ***interval model*** that considers that the model parameters θ are time-invariant but bounded by an interval set $\boldsymbol{\Theta} = \left\{\boldsymbol{\theta} \in \Re^{n\theta} \,\middle|\, \underline{\theta}_i \leqslant \theta_i \leqslant \overline{\theta}_i, i = 1, \cdots, n\theta\right\}$. This set represents the uncertainty about the exact knowledge of real system parameters $\tilde{\boldsymbol{\theta}}$. The interval for uncertain parameters can be inferred from real data using set-membership parameter estimation

[§] It is assumed that the system is in open-loop. The study of the effect of the loop is let a further research. Some preliminary results of effect of loop in the fault sensitivity analysis can be found in [19].

[¶] It should be noticed that $\boldsymbol{u}_0(k)$ is the real system input and does not have to be equal to the measured system input because the input sensor might be faulty or affected by noise.

algorithms [18]. Assuming that the system (1) is completely observable for all $\boldsymbol{\theta} \in \boldsymbol{\Theta}$, the following ***interval observer*** can be built as follows:

$$\begin{aligned}\hat{\boldsymbol{x}}(k+1,\boldsymbol{\theta}) &= (\boldsymbol{A}(\boldsymbol{\theta})-\boldsymbol{L}\boldsymbol{C}(\boldsymbol{\theta}))\hat{\boldsymbol{x}}(k,\boldsymbol{\theta})+\boldsymbol{B}(\boldsymbol{\theta})\boldsymbol{u}(k)+\boldsymbol{L}\boldsymbol{y}(k) = \boldsymbol{A}_o(\boldsymbol{\theta})\hat{\boldsymbol{x}}(k,\boldsymbol{\theta})+\boldsymbol{B}(\boldsymbol{\theta})\boldsymbol{u}(k)+\boldsymbol{L}\boldsymbol{y}(k)\\ \hat{\boldsymbol{y}}(k,\boldsymbol{\theta}) &= \boldsymbol{C}(\boldsymbol{\theta})\hat{\boldsymbol{x}}(k,\boldsymbol{\theta})\end{aligned} \tag{6}$$

where $\boldsymbol{u}(k)$ is the measured system input vector; $\hat{\boldsymbol{x}}(k,\boldsymbol{\theta})$and $\hat{\boldsymbol{y}}(k,\boldsymbol{\theta})$ meaning the estimated system space-state vector and the estimated system output vector for a given value of $\boldsymbol{\theta} \in \boldsymbol{\Theta}$, respectively. Noticing that the relation between the measured system, $\boldsymbol{u}(k)$, and the real system input, $\boldsymbol{u}_0(k)$, includes the effect of faults in the input sensors, and as result, the expression of $\boldsymbol{u}(k)$ can be written as follows:

$$\boldsymbol{u}(k) = \boldsymbol{u}_0(k) + \boldsymbol{F}_u(\boldsymbol{\theta})\boldsymbol{f}_u(k) \tag{7}$$

where $f_u(k) \in \Re^{nu}$ is the input sensor fault while $\boldsymbol{F}_u(\theta) \in \Re^{nu\times nu}$ is its associated matrix.

In the observation approach, the observer gain matrix, $\mathbf{L} \in \Re^{nx\times ny}$, is designed to guarantee the interval observer (6), is stable, and presents the desired performance regarding fault detection for all $\boldsymbol{\theta} \in \boldsymbol{\Theta}$using LMI pole placement [20]. The effect of the uncertain parameters θ on the observer temporal response $\hat{\boldsymbol{y}}(k,\boldsymbol{\theta})$gives a bounded interval which satisfies

$$y_i(k,\tilde{\boldsymbol{\theta}}) \in [\underline{\hat{y}}_i(k),\ \overline{\hat{y}}_i(k)] \tag{8}$$

in a non-faulty case. Such interval is computed independently for each output (neglecting couplings between outputs):

$$\underline{\hat{y}}_i(k) = \min_{\boldsymbol{\theta}\in\boldsymbol{\Theta}}(\hat{y}_i(k,\boldsymbol{\theta})) \text{ and } \bar{\hat{y}}_i(k) = \max_{\boldsymbol{\theta}\in\boldsymbol{\Theta}}(\hat{y}_i(k,\boldsymbol{\theta})) \tag{9}$$

subject to the observer equations given by (6). It can be computed using the algorithm based on numerical optimization presented in [21] or using zonotopes [9].

In [13], it was noticed that two particular cases could be distinguished in the observer model structure. First, the observer becomes a ***simulator*** when $\boldsymbol{L}$=$\boldsymbol{0}$ because the observer eigenvalues are those ones of the plant, but it can only be used when the system is stable. And second, the observer becomes a ***predictor*** when the observer gain ($\boldsymbol{L} = \boldsymbol{L}_p$)[‖] is selected such that all the observer eigenvalues are at the origin ('***deadbeat observer***') [15]. In this case, the fault indication given by this model has a minimum persistence, which depends on the order of the system (*weak fault detection*) [13]. As a consequence, a poor performance of the fault detection module causing a wrong fault diagnosis result may be obtained [22]. In line with the main conclusions of [13], when an observer is considered, the fault indication is more persistent for a certain value of $\boldsymbol{L}$ than the corresponding one to the *dead-beat observer*, and consequently, the observer model structure seems to be more suitable in order to enhance the fault detection performance of a certain model.

Alternatively, the observer given by (6) can be expressed in input-output form using the q-transform and considering zero initial conditions as it follows:

$$\hat{\boldsymbol{y}}(k,\boldsymbol{\theta}) = \boldsymbol{G}_o(q^{-1},\boldsymbol{\theta})\boldsymbol{u}(k) + \boldsymbol{H}_o(q^{-1},\boldsymbol{\theta})\boldsymbol{y}(k) \tag{10}$$

where

$$\boldsymbol{G}_o(q^{-1},\boldsymbol{\theta}) = \boldsymbol{C}(\boldsymbol{\theta})(\boldsymbol{I}-q^{-1}\boldsymbol{A}_o(\boldsymbol{\theta}))^{-1}\boldsymbol{B}(\boldsymbol{\theta})q^{-1} \tag{11}$$

$$\boldsymbol{H}_o(q^{-1},\boldsymbol{\theta}) = \boldsymbol{C}(\boldsymbol{\theta})(\boldsymbol{I}-q^{-1}\boldsymbol{A}_o(\boldsymbol{\theta}))^{-1}\boldsymbol{L}q^{-1} \tag{12}$$

The sub index 'o' indicates the input/output functions associated with the observer model.

[‖] When $\boldsymbol{C}$ has an inverse, the observer structure forces the predictor approach to satisfy $\boldsymbol{L}_p\boldsymbol{C} = \boldsymbol{A}$.

2.3. Interval predictor

On the other hand, the system described by (1) could be also monitored using a linear interval *predictor* with the following structure

$$\hat{\boldsymbol{y}}(k,\boldsymbol{\theta}) = \boldsymbol{A}_p(q^{-1},\boldsymbol{\theta})\boldsymbol{y}(k) + \boldsymbol{B}_p(q^{-1},\boldsymbol{\theta})\boldsymbol{u}(k) \tag{13}$$

where matrices $\boldsymbol{A}_p(q^{-1},\boldsymbol{\theta}) \in \Re^{ny\times ny}$ and $\boldsymbol{B}_p(q^{-1},\boldsymbol{\theta}) \in \Re^{ny\times nu}$ are polynomial matrices of q^{-1}, where each polynomial has $n\theta$ uncertain coeficients defined such as it was carried out in the previous section ($\boldsymbol{\theta} \in \boldsymbol{\Theta}, \boldsymbol{\Theta} = \left\{\boldsymbol{\theta} \in \Re^{n\theta} \middle| \underline{\theta}_i \leqslant \theta_i \leqslant \overline{\theta}_i, i = 1,\cdots,n\theta\right\}$). Using the method given by [5], the predictor of minimum order is obtained, which behaves like an observer when the condition $\boldsymbol{L} = \boldsymbol{L}_p$ is satisfied. According to [15], the fault indication given by this type of predictor has a minimum persistence (*weak fault detection*). Considering this drawback, this paper focuses on obtaining a λ-order predictor, which behaves like an observer for a given value of $\boldsymbol{L}$. This method can be viewed as a generalization of the approaches given by [15] and [6].

Equivalently, the predictor given by (13) can also be expressed in input-output form using the shift operator q^{-1} and assuming zero initial conditions

$$\hat{\boldsymbol{y}}(k,\boldsymbol{\theta}) = \boldsymbol{G}_p(q^{-1},\boldsymbol{\theta})\boldsymbol{u}(k) + \boldsymbol{H}_p(q^{-1},\boldsymbol{\theta})\boldsymbol{y}(k) \tag{14}$$

where comparing the structure of (14) with (13)

$$\boldsymbol{G}_p(q^{-1},\boldsymbol{\theta}) = \boldsymbol{B}_p(q^{-1},\boldsymbol{\theta})q^{-1} \tag{15}$$

$$\boldsymbol{H}_p(q^{-1},\boldsymbol{\theta}) = \boldsymbol{A}_p(q^{-1},\boldsymbol{\theta})q^{-1} \tag{16}$$

and the sub index 'p' indicates the polynomial matrices that are associated with the predictor model.

2.4. Equivalence between λ -order interval predictors and interval observers

Iterating the observer equation (6) k times forward, starting from $k = 0$, the predicted output at time k can be determined as (see more details, e.g., in [23])

$$\hat{\boldsymbol{y}}(k,\boldsymbol{\theta}) = \boldsymbol{C}(\boldsymbol{\theta})\boldsymbol{A}_o(\boldsymbol{\theta})^k\hat{\boldsymbol{x}}(0) + \sum_{v=1}^{k}\boldsymbol{C}(\boldsymbol{\theta})\boldsymbol{A}_o(\boldsymbol{\theta})^{v-1}\boldsymbol{B}(\boldsymbol{\theta})\boldsymbol{u}(k-v) + \sum_{v=1}^{k}\boldsymbol{C}(\boldsymbol{\theta})\boldsymbol{A}_o(\boldsymbol{\theta})^{v-1}\boldsymbol{L}\boldsymbol{y}(k-v) \tag{17}$$

for every value of $\boldsymbol{\theta} \in \boldsymbol{\Theta}$.

The current estimated output not only depends on the initial state but also on the last k measurements of the system inputs and outputs. The contribution of the states depends on the dynamics of the observer and as a result, if k is large enough, the contribution of the initial state $\hat{\boldsymbol{x}}(0)$ to the output estimation $\hat{\boldsymbol{y}}(k)$ can be dismissed. If it is possible to find a number of samples λ such that for $k > \lambda$ (see *Proposition 1*, later on)

$$\boldsymbol{A}_o(\boldsymbol{\theta})^k = (\boldsymbol{A}(\boldsymbol{\theta}) - \boldsymbol{L}\boldsymbol{C}(\boldsymbol{\theta}))^k \approx 0 \quad \forall\boldsymbol{\theta} \in \boldsymbol{\Theta} \tag{18}$$

is satisfied, it can be said that the dynamics of the observer has vanished. Then, the predicted output can be approximated through

$$\hat{\boldsymbol{y}}(k,\boldsymbol{\theta}) \approx \left[\sum_{v=1}^{\lambda}\boldsymbol{C}(\boldsymbol{\theta})\boldsymbol{A}_o(\boldsymbol{\theta})^{v-1}\boldsymbol{B}(\boldsymbol{\theta})q^{-(v-1)}\right]\boldsymbol{u}(k-1) + \left[\sum_{v=1}^{\lambda}\boldsymbol{C}(\boldsymbol{\theta})\boldsymbol{A}_o(\boldsymbol{\theta})^{v-1}\boldsymbol{L}q^{-(v-1)}\right]\boldsymbol{y}(k-1) \tag{19}$$

which has the same structure as the predictor expression given by (13). Therefore, this especial interval observer, where the contribution of the initial $\hat{\boldsymbol{x}}(0)$ can be obviated if the relation (18)

is satisfied, can be seen as a interval predictor of order λ, which computes at every time instant, roughly, the same system output estimation interval. Comparing (13) with (19), the matrices of the predictor model related to those ones of the interval observer are obtained resulting[**]

$$\boldsymbol{A}_p(q^{-1},\boldsymbol{\theta}) = \sum_{v=1}^{\lambda} \boldsymbol{C}(\boldsymbol{\theta})\boldsymbol{A}_o(\boldsymbol{\theta})^{v-1}\boldsymbol{L}q^{-(v-1)} \tag{20}$$

$$\boldsymbol{B}_p(q^{-1},\boldsymbol{\theta}) = \sum_{v=1}^{\lambda} \boldsymbol{C}(\boldsymbol{\theta})\boldsymbol{A}_o(\boldsymbol{\theta})^{v-1}\boldsymbol{B}(\boldsymbol{\theta})q^{-(v-1)} \tag{21}$$

The inspection of these equations shows that the relationship between the interval observer and the interval predictor scheme is given in terms of the observer matrix $\boldsymbol{A}_o$, which depends on the observer gain matrix $\boldsymbol{L}$. This gain not only determines the observer behavior but also the order λ of the equivalent predictor (18). The interval predictor given by (19) is a ***closed-loop predictor*** because it uses measurements of past system inputs and outputs to predict the present system output.

From (19), it follows that when the particular case of $\boldsymbol{L} = \boldsymbol{0}$ (simulator approach) is considered, the predictor given by (19) becomes an ***open-loop predictor*** that only uses measurements of past system inputs to predict the present system output.

In order to derive analytically the order λ of the equivalent interval predictor to a given interval observer, the following proposition can be used:

Proposition 1
Let us consider that the interval observer given by (6) is asymptotic stable. Then, for a $k > \lambda_\varepsilon$, (18) can be approximated with a desired degree of approximation ε

$$\left\| \boldsymbol{A}_o(\boldsymbol{\theta})^k \right\|_\infty = \left\| [\boldsymbol{A}(\boldsymbol{\theta}) - \boldsymbol{L}\boldsymbol{C}(\boldsymbol{\theta})]^k \right\|_\infty < \varepsilon \approx 0 \forall \boldsymbol{\theta} \in \boldsymbol{\Theta} \tag{22}$$

and consequently, λ_ε is also the order of the predictor (19):

$$\lambda_\varepsilon = \max_{\boldsymbol{\theta}\in\boldsymbol{\Theta}} \left[\frac{|log\varepsilon| + log\kappa(\boldsymbol{\theta})}{|log\rho(\boldsymbol{\theta})|} \right] \tag{23}$$

where ρ is the spectral radius of the interval observer matrix $\boldsymbol{A}_o$ determined by the maximum absolute value of all the eigenvalues of this matrix and κ is the condition number[††] of $\boldsymbol{A}_o$.

Proof
See Appendix the proof inspired in results presented in [21]. □

Thus, (23) allows to obtain the lower order of the equivalent predictor for a given observer gain matrix $\boldsymbol{L}$ and precision ε. When the observer gain matrix $\boldsymbol{L}$ tends to $\boldsymbol{L}_p$ (i.e., to the *'dead-beat observer'*), the observer poles tend to zero and, consequently, so does the spectral radius. Then, according to (23), λ_ε tends to decrease its values. When $\boldsymbol{L}$=$\boldsymbol{L}_p$, ρ tends to zero what provokes λ_ε to tend to its minimum value given by the system order. Otherwise, when $\boldsymbol{L}$=$\boldsymbol{0}$, the observer becomes a simulator, and ρ tends to its maximum value given by one, and thus, λ_ε tends to an infinite value.

[**] Equations (20) and (21) can also be derived from Von Neumann expansion of $(\boldsymbol{I} - q^{-1}\boldsymbol{A}_o(\boldsymbol{\theta}))^{-1}$

[††] The condition number κ is determined by the result of the following matrix product: $\|\boldsymbol{T}_o\|.\|\boldsymbol{T}_o^{-1}\|$where $\boldsymbol{A}_o = \boldsymbol{T}\boldsymbol{\Lambda}_o\boldsymbol{T}^{-1}$. A matrix with a high κ is said to be ill-conditioned; otherwise, it is considered well conditioned.

2.5. Computational complexity

Puig *et al.* [17] illustrates that the problem of interval observation can be translated to an interval simulation. As it is noticed by [6], interval simulation requires a high computation cost at each sample time (*trajectory-based algorithm*), being generally incompatible with the real-time constraint needed by the fault detection module when applied to complex dynamic system. To avoid this computational drawbacks, except for some particular cases, the recurrence leads to replace state-space value sets by simpler outer value sets, such as boxes or ellipsoids what yields some over-estimations (*set-based algorithms*). The propagation of these approximations using this type of algorithms induces an accumulation of errors leading to an explosion of the computed sets (*wrapping effect*) [17, 24]. On the other hand, checking on a finite horizon, such as parity space approach does, avoids this drawback because it only needs system inputs and outputs to compute the output prediction to generate. However, as noticed in previous section, parity space approach produces a minimum order predictor [15] that has a response equivalent to a *'dead-beat observer'*. Thus, as it is known [7], when applied to fault detection, the minimum order predictor (or *'dead-beat observer'*) is highly sensitive to noise and, depending on the fault, only indicates the fault at its occurrence time instant. Conversely, observer models through the observer gain can filter noise and indicate the fault presence for longer time [13]. This motivates the use of higher order predictors with a fault detection performance equivalent to the behavior of an observer. However, computational complexity still remains because optimization problems related to compute a higher-order predictor equivalent to a given observer are nonlinear regarding the parameters (*trajectory-based algorithms*). Then, in order to guarantee the tightest interval bounding output prediction, a global optimization algorithm should be used because the optimization problem is non-convex. The only case in which such computational complexity can be reduced is when higher order predictor comes from an observer whose matrix $\boldsymbol{A}_o(\boldsymbol{\theta})$ has all elements positive and uncertain parameters enter in a linear way. In this case, the estimation interval for each system output prediction can be obtained evaluating the model uncertain parameters using two point-wise sets determined by their lower and upper interval bound ($\bar{\hat{y}}_i(k) = \hat{y}_i(k, \bar{\boldsymbol{\theta}})$ and $\underline{\hat{y}}_i(k) = \hat{y}_i(k, \underline{\boldsymbol{\theta}})$) [25–27]. Then, the equivalent λ-order predictor interval output can also be computed using these two known point-wise trajectories as (23) forces each observer trajectory to be equivalent to the associated predictor trajectory. In this case, the output estimation generated by the equivalent interval observer would also be computationally cheap because a set propagation-based approach (*set-based algorithm*) can be applied. This is because in this case, the interval observer is unaffected by the wrapping effect [17]. Besides, it should be taken into account that the elements of $\boldsymbol{A}_o(\boldsymbol{\theta})$ can be forced to be positive through the observer gain matrix $\boldsymbol{L}$ [24]. Thus, because the wrapping effect could be avoided by appropriately tuning the interval observer [17], we can find an equivalent $\lambda-$order interval predictor such that it also avoids the wrapping effect.

3. APPLICATION TO FAULT DETECTION

3.1. Residual generation and evaluation

Fault detection is based on calculating at every time instant a residual comparing the measurements of physical variables $\boldsymbol{y}(k)$ associated with the monitored system with their estimation $\hat{\boldsymbol{y}}(k, \boldsymbol{\theta})$ provided by the associated system model:

$$\boldsymbol{r}(k, \boldsymbol{\theta}) = \boldsymbol{y}(k) - \hat{\boldsymbol{y}}(k, \boldsymbol{\theta}) \tag{24}$$

where $\boldsymbol{r}(k, \boldsymbol{\theta}) \in \Re^{ny}$ is the residual set. According to [3], the ***computational form*** of the residual generator is given by the following:

$$\boldsymbol{r}(k, \boldsymbol{\theta}) = \boldsymbol{V}(q^{-1}, \boldsymbol{\theta})\boldsymbol{u}(k) + \boldsymbol{O}(q^{-1}, \boldsymbol{\theta})\boldsymbol{y}(k) \tag{25}$$

where $\boldsymbol{V}(q^{-1}, \theta)$ and $\boldsymbol{O}(q^{-\mathbf{1}}, \theta)$ are polynomial functions of the delay operator q^{-1}.

When the interval observer model is considered, the functions $\boldsymbol{V}(q^{-1}, \theta)$ and $\boldsymbol{O}(q^{-1}, \theta)$ can be obtained using its system output estimation (10) and the residual definition (24) what results in the following:

$$\boldsymbol{V}_o(q^{-1}, \boldsymbol{\theta}) = -\boldsymbol{G}_o(q^{-1}, \boldsymbol{\theta}) = -\boldsymbol{C}(\boldsymbol{\theta})(\boldsymbol{I} - q^{-1}\boldsymbol{A}_o(\boldsymbol{\theta}))^{-1}\boldsymbol{B}(\boldsymbol{\theta})q^{-1} \tag{26}$$

$$\boldsymbol{O}_o(q^{-1}, \boldsymbol{\theta}) = \boldsymbol{I} - \boldsymbol{H}_o(q^{-1}, \boldsymbol{\theta}) = \boldsymbol{I} - \boldsymbol{C}(\boldsymbol{\theta})(\boldsymbol{I} - q^{-1}\boldsymbol{A}_o(\boldsymbol{\theta}))^{-1}\boldsymbol{L}q^{-1} \tag{27}$$

In the interval predictor case, the model system output estimation is given by (14), and consequently, those input/output polynomial functions are determined by the following expressions:

$$\boldsymbol{V}_p(q^{-1}, \boldsymbol{\theta}) = -\boldsymbol{G}_p(q^{-1}, \boldsymbol{\theta}) = -\boldsymbol{B}_p(q^{-1}, \boldsymbol{\theta})q^{-1} \tag{28}$$

$$\boldsymbol{O}_p(q^{-1}, \boldsymbol{\theta}) = \boldsymbol{I} - \boldsymbol{H}_p(q^{-1}, \boldsymbol{\theta}) = (\boldsymbol{I} - \boldsymbol{A}_p(q^{-1}, \boldsymbol{\theta})q^{-1}) \tag{29}$$

Alternatively, the residual computational form (25) can be also expressed in terms of the effects caused by faults using its ***internal*** or ***unknown-input-effect form*** [3]. This form is obtained applying the expressions of the system output (2) and input (7) to the residual computational form (25):

$$\begin{aligned}\boldsymbol{r}(k, \boldsymbol{\theta}) = \boldsymbol{r}_0(k, \boldsymbol{\theta}) + \left(\boldsymbol{I} - \boldsymbol{H}(q^{-1}, \boldsymbol{\theta})\right)\left(\boldsymbol{G}_{fa}(q^{-1}, \tilde{\boldsymbol{\theta}})\boldsymbol{f}_a(k) + \boldsymbol{G}_{fy}(q^{-1}, \tilde{\boldsymbol{\theta}})\boldsymbol{f}_y(k)\right) \\ - \boldsymbol{G}(q^{-1}, \boldsymbol{\theta})\boldsymbol{F}_u(\boldsymbol{\theta})\boldsymbol{f}_u(k)\end{aligned} \tag{30}$$

where

$$\boldsymbol{r}_0(k, \boldsymbol{\theta}) = -\boldsymbol{G}(q^{-1}, \boldsymbol{\theta})\boldsymbol{u}_0(k) + \left(\boldsymbol{I} - \boldsymbol{H}(q^{-1}, \boldsymbol{\theta})\right)\boldsymbol{y}_0(k) \tag{31}$$

would be the expression of the non-faulty residual, which is just due to parametric uncertainty, $\boldsymbol{\theta} \in \boldsymbol{\Theta}$. Notice that in (30), it appears both the unknown system parameters $\tilde{\boldsymbol{\theta}}$ and uncertain variable $\boldsymbol{\theta} \in \boldsymbol{\Theta}$Morevoer, in (30), the polynomial functions $\boldsymbol{H}(q^{-1}, \boldsymbol{\theta})$ and $\boldsymbol{G}(q^{-1}, \boldsymbol{\theta})$ are determined by $\boldsymbol{H}_o(q^{-1}, \boldsymbol{\theta})$ (12) and $\boldsymbol{G}_o(q^{-1}, \boldsymbol{\theta})$ (11) when considering the observer case or by $\boldsymbol{H}_p(q^{-1}, \boldsymbol{\theta})$(16) and $\boldsymbol{G}_p(q^{-1}, \boldsymbol{\theta})$ (15) when considering the predictor case.

In the fault detection and fault isolation interface used in [28], the residual (24) is computed regarding the nominal observer model $\hat{\boldsymbol{y}}^o(k)$ obtained using the observer parameter set $\boldsymbol{\theta} = \boldsymbol{\theta}^o \in \boldsymbol{\Theta}$,

$$\boldsymbol{r}^o(k) = \boldsymbol{y}(k) - \hat{\boldsymbol{y}}^o(k) \tag{32}$$

It must be taken into account that when considering model uncertainty located in parameters, the residual generated by (32) will not be zero even in a non-faulty scenario. In this case, the possible values of each component of this residual vector, $\boldsymbol{r}^o(k)$, can be bounded using the following interval (neglecting couplings among outputs), such as illustrated by [7]:

$$[\underline{r}_i^o(k), \overline{r}_i^o(k)] \tag{33}$$

where

$$\underline{r}_i^o(k) = \hat{y}_i(k) - \hat{y}_i^o(k) \text{ and } \bar{r}_i^o(k) = \bar{\hat{y}}_i(k) - \hat{y}_i^o(k) \tag{34}$$

being $\underline{\hat{y}}_i(k)$ and $\bar{\hat{y}}_i(k)$ the bounds of the ith-system output estimation computed using the interval observer (6) or its equivalent interval predictor (19) and obtained according to (10).

In this case, this residual interval constitutes the ***adaptive threshold*** because the comparison of every component of the nominal residual vector, $r_i^o(k)$, with its corresponding bounding interval (33) allows the indication of the fault if the following relation is satisfied

$$r_i^o(k) \notin [\underline{r}_i^o(k), \overline{r}_i^o(k)] \tag{35}$$

While the fault detection test given by (35) is fulfilled, the fault can be indicated.

3.2. *Equivalence between the interval observer and its associated interval predictor regarding fault indication*

As it was mentioned in the previous section, the indication of a fault by the fault detection stage is just determined by the test given by (35). Thus, two models (interval observer and its equivalent $\lambda-$order predictor), which generate at every time instant the same residual $r_i^o(k)$ having the same adaptive threshold $[\underline{r}_i^o(k), \overline{r}_i^o(k)]$, will indicate the fault equivalently.

According to (23), which sets the order of the equivalent predictor to the given interval observer, the system output estimations computed by both models fulfil the following condition:

$$\left\| \hat{\boldsymbol{y}}_o(k, \boldsymbol{\theta}) - \hat{\boldsymbol{y}}_p(k, \boldsymbol{\theta}) \right\| \approx 0 \quad \forall \boldsymbol{\theta} \in \boldsymbol{\Theta} \tag{36}$$

where the sub index o is set for the observer model while sub index p for the equivalent predictor model.

Therefore, according to the residual expression given by (24), the residuals generated by both models also fulfil an equivalent condition:

$$\left\| \boldsymbol{r}_o(k, \boldsymbol{\theta}) - \boldsymbol{r}_p(k, \boldsymbol{\theta}) \right\| \approx 0 \quad \forall \boldsymbol{\theta} \in \boldsymbol{\Theta} \tag{37}$$

Then, considering the conditions given by (36) and (37), the observer and its equivalent predictor are generating at every time instant the same residual $r_i^o(k)$ and the same adaptive threshold $[\underline{r}_i^o(k), \overline{r}_i^o(k)]$, and consequently, both models have an equivalent performance regarding the fault indication.

3.3. *Sensitivity of the residual to a fault*

According to [3], the ***sensitivity of the residual*** to a fault is given by

$$\boldsymbol{S_f} = \frac{\partial \boldsymbol{r}}{\partial \boldsymbol{f}} \tag{38}$$

which leads to obtain the function that describes the effect on the residual, $\boldsymbol{r}$, of a given fault $\boldsymbol{f}$. In [13], the concept of the residual sensitivity to a fault was recalled extending this concept to interval observers focusing on the dynamical aspects of this model property. Thereby, a complete analysis regarding the influence of the observer gain $\boldsymbol{L}$ on the time evolution of this property was carried out considering output sensor faults $\boldsymbol{f}_y$, input sensor faults $\boldsymbol{f}_u$, and actuator faults $\boldsymbol{f}_a$. According to [3] regarding non-interval models and [13] regarding interval observer models, the fault residual sensitivity is a key property of the considered model concerning its fault detection performance as it determines the adaptive threshold, the minimum detectable fault, and the time a fault is indicated.

As illustrated in [13], analyzing the residual ***internal form*** given by (30), and considering the fault residual sensitivity definition given by (38), the residual sensitivity for the case of an output sensor fault $\boldsymbol{f}_y$ is given by a matrix $\boldsymbol{S}_{fy}$ of dimension $ny \times ny$ whose expression is as follows:

$$\boldsymbol{S}_{fy}(q^{-1}, \boldsymbol{\theta}) = \boldsymbol{O}(q^{-1}, \boldsymbol{\theta}) \boldsymbol{G}_{fy}(q^{-1}, \tilde{\boldsymbol{\theta}}) = \left(\boldsymbol{I} - \boldsymbol{H}(q^{-1}, \boldsymbol{\theta}) \right) \boldsymbol{G}_{fy}(q^{-1}, \tilde{\boldsymbol{\theta}}) \tag{39}$$

Applying the same procedure, the residual sensitivity to an input sensor fault $\boldsymbol{f}_u$ is given by a matrix $\boldsymbol{S}_{fu}$ of dimension $ny \times nu$, and the residual sensitivity to an actuator fault $\boldsymbol{f}_a$ is given by a matrix $\boldsymbol{S}_{fa}$of dimension $ny \times nu$ whose expressions are as follows:

$$\boldsymbol{S}_{fu}(q^{-1}, \boldsymbol{\theta}) = \boldsymbol{V}(q^{-1}, \boldsymbol{\theta}) \boldsymbol{F}_u(\boldsymbol{\theta}) = -\boldsymbol{G}(q^{-1}, \boldsymbol{\theta}) \boldsymbol{F}_u(\boldsymbol{\theta}) \tag{40}$$

$$\boldsymbol{S}_{fa}(q^{-1}, \boldsymbol{\theta}) = \boldsymbol{O}(q^{-1}, \boldsymbol{\theta}) \boldsymbol{G}_{fa}(q^{-1}, \tilde{\boldsymbol{\theta}}) = \left(\boldsymbol{I} - \boldsymbol{H}(q^{-1}, \boldsymbol{\theta}) \right) \boldsymbol{G}_{fa}(q^{-1}, \tilde{\boldsymbol{\theta}}) \tag{41}$$

Notice that in residuals fault sensitivities (39) and (41), the uncertain model parameter $\boldsymbol{\theta}$ and unknown system parameter $\tilde{\boldsymbol{\theta}}$ appear.

Table I. Fault residual sensitivity dynamics[‡‡].

	Simulation $\boldsymbol{L=0}$ *or* $\lambda \to \infty$	***Observation*** $\boldsymbol{L=L_o}$ *or* $n < \lambda < \infty$	***Prediction***[§§] $\boldsymbol{L=L_p}$ *or* $\lambda = n$
$\mathbf{S}_{fy}$	Constant	Pulse	Deadbeat
$\mathbf{S}_{fu}$	Dynamic response	Dynamic response	Constant
$\mathbf{S}_{fa}$	Dynamic response	Dynamic response	Constant

As pointed out in [13], it is important to notice how the fault residual sensitivity concept (38) determines the value of the residual at each time instant when the monitored system is affected by a fault. Thus, the residual expression can be rewritten as follows considering the residual internal form given by (30) and the residual sensitivity to an output sensor fault, $\boldsymbol{S}_{fy}$, (39), to an input sensor fault, $\boldsymbol{S}_{fu}$, (40), and to an actuator, $\boldsymbol{S}_{fa}$, (41):

$$\boldsymbol{r}(k,\boldsymbol{\theta}) = \boldsymbol{r}_0(k,\boldsymbol{\theta}) + \boldsymbol{S}_{fa}(q^{-1},\boldsymbol{\theta})\boldsymbol{f}_a(k) + \boldsymbol{S}_{fy}(q^{-1},\boldsymbol{\theta})\boldsymbol{f}_y(k) + \boldsymbol{S}_{fu}(q^{-1},\boldsymbol{\theta})\boldsymbol{f}_u(k) \tag{42}$$

As noticed by [3] and [2], this equation let us understand the importance of the fault residual sensitivity to indicate the fault taking into account that a fault is detected while test (35) is satisfied.

In this section, it will be demonstrated that interval observers and their equivalent λ-order predictors must have the same residual sensitivity to whatever kind of fault affecting to the monitored system. The residual internal form given by (42) determines that the value of the residual at every time instant is given by the disturbance caused by different faults, which can affect the monitored system (actuator fault, $\boldsymbol{f}_a$, output sensor fault, $\boldsymbol{f}_y$, and input sensor fault, $\boldsymbol{f}_u$) and the disturbance caused by the model uncertainty. This residual form shows that the residual disturbance caused by a fault vector is determined using the residual sensitivity to this kind of fault ($\boldsymbol{S}_{fy}$, (39); $\boldsymbol{S}_{fu}$, (40); and $\boldsymbol{S}_{fa}$, (41)) while the residual disturbance caused by the model uncertainty is given by $\boldsymbol{r}_0$ (31). Then, considering the monitored system is affected by a fault vector $\boldsymbol{f}$ whose occurrence time instant is t_0, the expression of the residual according to (42) will be given by

$$\boldsymbol{r}(k,\boldsymbol{\theta}) = \begin{cases} \boldsymbol{r}_0(k,\boldsymbol{\theta}) + \boldsymbol{S}_f(q^{-1},\boldsymbol{\theta})\boldsymbol{f}(k)q^{-t_0}k \geq t_0 \\ \boldsymbol{r}_0(k,\boldsymbol{\theta}) \qquad\qquad k < t_0 \end{cases} \tag{43}$$

where $\boldsymbol{S}_f$ is the residual sensitivity to the fault vector $\boldsymbol{f}$. Then, according to (37), at whatever time instant k, the interval observer and its equivalent predictor generate the same residual (37). As a result of this statement and derived from (43), it is concluded both approaches must have the same residual sensitivity to the fault vector $\boldsymbol{f}$ if condition (23) is satisfied. This equivalence can be written as it follows:

$$\boldsymbol{S}_{of}(q^{-1},\boldsymbol{\theta}) \approx \boldsymbol{S}_{pf}(q^{-1},\boldsymbol{\theta}) \forall \boldsymbol{\theta} \in \boldsymbol{\Theta} \tag{44}$$

where the sub index o is set for the observer model while sub index p for the equivalent predictor model.

This result shows that such as [13] illustrates that the fault residual sensitivity dynamics can be described regarding the observation gain $\boldsymbol{L}$, the same sensitivity dynamics can also be achieved with the equivalent predictor calculating its order using (23). In the following, Table I describes the sensitivity dynamics in terms of $\boldsymbol{L}$ and λ such as it was carried out in terms of $\boldsymbol{L}$ in [13]. This allows to use the same design guidelines for the interval predictor that those used for interval observers presented in [7].

[‡‡] $\boldsymbol{n}$ stands for the predictor minimum order

[§§] Predictor of minimum order ("dead-beat observer").

Figure 1. DAMADICS smart actuator. [Colour figure can be viewed at wileyonlinelibrary.com]

4. APPLICATION EXAMPLE

4.1. Description

The application example proposed to illustrate the obtained results deals with an industrial smart actuator, which has been proposed as an FDI benchmark in the context of the European research training network DAMADICS (Figure 1). This smart actuator is used in the evaporation station of a sugar factory in Poland, and it consists in a control valve, a pneumatic servomotor, and a smart positioner [29] (Figure 2).

Using the benchmark described in [29] as a real plant and a mixed optimization-identification algorithm as in [30], the following linear interval model of the actuator valve position has been derived [7]:

$$\begin{aligned} \hat{\boldsymbol{x}}(k+1,\boldsymbol{\theta}) &= \boldsymbol{A}(\boldsymbol{\theta})\hat{\boldsymbol{x}}(k) + \boldsymbol{B}(\boldsymbol{\theta})\boldsymbol{u}(k) \\ \hat{\boldsymbol{y}}(k,\boldsymbol{\theta}) &= \boldsymbol{C}(\boldsymbol{\theta})\hat{\boldsymbol{x}}(k) \end{aligned} \tag{45}$$

with: $\hat{\boldsymbol{x}}(k) = \left[\, \hat{x}_1(k)\ \hat{x}_2(k)\ \hat{x}_3(k) \,\right]^{\mathrm{t}}$, $\boldsymbol{A}(\boldsymbol{\theta}) = \begin{bmatrix} 0 & 0 & \theta_3 \\ 1 & 0 & \theta_2 \\ 0 & 1 & \theta_1 \end{bmatrix}$, $\boldsymbol{B}(\boldsymbol{\theta}) = \begin{bmatrix} 0 \\ 0 \\ \theta_4 \end{bmatrix}$, $\boldsymbol{C}(\boldsymbol{\theta}) = \left[\, 0\ 0\ 1 \,\right]$ and $\boldsymbol{u}(k) = CVP(k-2)$ where $\hat{x}_3(k)$ is the valve position (X in Figure 2) estimation, $\hat{\boldsymbol{y}}(k,\boldsymbol{\theta})$ is the estimation of this position (PV in Figure 2) measured (in Volt) by the displacement transducer (DT in Figure 2), and $CVP(k)$ (CVI in Figure 2) is the command pressure (in Pascal) measured by a given input sensor. Then, concerning the model uncertain parameters, they are bounded by their uncertainty intervals: $\theta_1 \in [1.1417\ 1.1471]$, $\theta_2 \in [0.3995\ 0.4103]$, $\theta_3 \in [-0.5537\ -0.5484]$, and $\theta_4 \in$ [2.180e-4 2.183e-4] while their nominal values are given by θ_1^o =1.1444, θ_2^o =0.4049, $\theta_3^o = -0.5510$, and θ_4^o =2.182e-4. Regarding the command pressure, a constant value given by $u(k) = 1Pa$ has been considered.

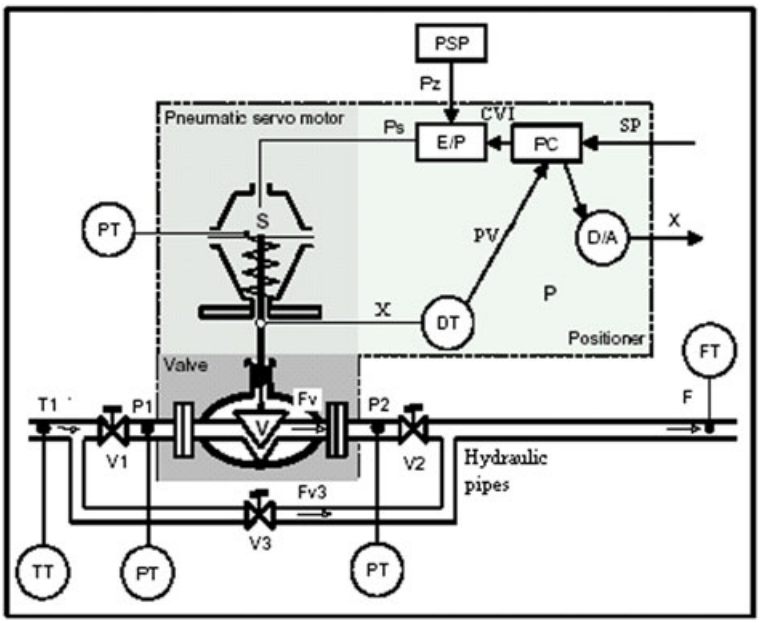

Figure 2. DAMADICS smart actuator block diagram. [Colour figure can be viewed at wileyonlinelibrary.com]

4.2. *Output estimation and residual analysis*

According to (10), the observer estimation interval of the system output $\left[\underline{\hat{\boldsymbol{y}}}(k), \overline{\hat{\boldsymbol{y}}}(k)\right]$ can be obtained from (45) considering the following observer gain matrix $\boldsymbol{L} = [l_3, l_2, l_1]^{\mathrm{t}}$:

$$\begin{aligned}\hat{\boldsymbol{y}}(k,\boldsymbol{\theta}) &= \boldsymbol{G}_o(q^{-1},\boldsymbol{\theta})\boldsymbol{u}(k) + \boldsymbol{H}_o(q^{-1},\boldsymbol{\theta})\boldsymbol{y}(k) = \\ &= \frac{\theta_4 q^{-1}}{1+(l_1-\theta_1)q^{-1}+(l_2-\theta_2)q^{-2}+(l_3-\theta_3)q^{-3}}\boldsymbol{u}(k) \\ &\quad + \frac{l_1 q^{-1}+l_2 q^{-2}+l_3 q^{-3}}{1+(l_1-\theta_1)q^{-1}+(l_2-\theta_2)q^{-2}+(l_3-\theta_3)q^{-3}}\boldsymbol{y}(k)\end{aligned} \tag{46}$$

where l_1, l_2, and l_3 are the observer gains. The residual expression can be inferred from (25), (26), and (27) using (46):

$$\begin{aligned}\boldsymbol{r}(k,\boldsymbol{\theta}) &= \boldsymbol{V}_o(q^{-1},\boldsymbol{\theta})\boldsymbol{u}(k) + \boldsymbol{O}_o(q^{-1},\boldsymbol{\theta})\boldsymbol{y}(k) = \left(-\boldsymbol{G}_o(q^{-1},\boldsymbol{\theta})\right)\boldsymbol{u}(k) + \left(\boldsymbol{I} - \boldsymbol{H}_o(q^{-1},\boldsymbol{\theta})\right)\boldsymbol{y}(k) = \\ &= -\frac{\theta_4 q^{-1}}{1+(l_1-\theta_1)q^{-1}+(l_2-\theta_2)q^{-2}+(l_3-\theta_3)q^{-3}}\boldsymbol{u}(k) \\ &\quad + \frac{1-\theta_1 q^{-1}-\theta_2 q^{-2}-\theta_3 q^{-3}}{1+(l_1-\theta_1)q^{-1}+(l_2-\theta_2)q^{-2}+(l_3-\theta_3)q^{-3}}\boldsymbol{y}(k)\end{aligned} \tag{47}$$

According to [25], because the state-space matrix $\boldsymbol{A}(\boldsymbol{\theta})$ of the application example model (45) does not fulfil the positivity property, its associated interval observer model (46) suffers from the *wrapping effect* when the output interval $\left[\underline{\hat{\boldsymbol{y}}}(k), \overline{\hat{\boldsymbol{y}}}(k)\right]$ is computed iteratively from the output intervals obtained in previous time instants (*set-based approach)*. See Section 2.5 for more details. However, [24] establishes that the wrapping effect may be avoided if the positive condition[¶¶] is

[¶¶] The positive condition presented in [24] forces the interval observer matrix to satisfy the positive property zero-valuing its negative elements using the observer gain.

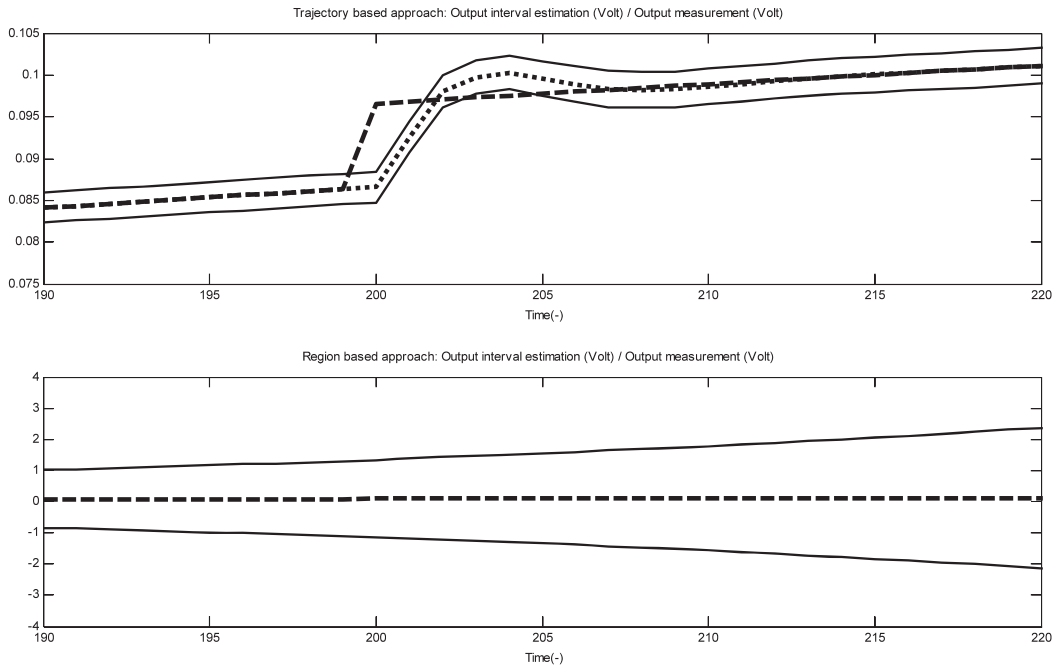

Figure 3. Time evolution of the system output estimation interval *(solid line)*, its nominal value *(dot line)*, and the system output sensor measurement *(dash line)* using a trajectory and set-based algorithm.

forced using the observer gain $\boldsymbol{L}$. Thereby, according to [24], the positivity condition related to the considered application example can be expressed as follows:

$$l_3 = \theta_3 \tag{48}$$

which using the observer gain parameterization[IIII] $l_i = \alpha_i \theta_i$ implies $\alpha_3 = 1$. In case, if the condition given by (48) is not forced, the output estimation computed by the interval observer should be obtained using a *trajectory-based algorithm* [17] or, according to Section 2.3, using its equivalent λ-order interval predictor as both approaches estimate the same system output interval according to (36).

To illustrate the benefit of using a *trajectory-based algorithm* for propagating uncertainty instead of a *set-based approach*, let us assume a constant additive fault affecting the system output sensor occurring at time instant $t_0 = 200$ and whose value is given by $f = 0.01$ V (roughly, *10%* of the steady-state system output nominal value), and let us also consider an observation gain set determined by $\alpha_1 = \alpha_2 = \alpha_3 = 0.5$. Note that in this case, the wrapping effect is not avoided because (48) is not satisfied. Thus, the positivity condition of the interval observer matrix will not be sastified, and the set-based approach will suffer from the wrapping effect. This is illustrated in Figure 3 where the time evolution of the estimated system output interval (*solid line*), nominal values (*dot line*), and the output sensor measurement (*dash line*) are plotted between the time instants $t_1 = 190$ and $t_2 = 220$ using the interval observer input-output form given by (46) and considering a *trajectory-based algorithm* (*upper plot*) and a *set-based algorithm* (*lower plot*). Thus, according to the mentioned Section 2.5, while the trajectory-based approach produces an accurate interval what allows to detect the fault, the corresponding interval produced using a set-based approach is useless because of the wrapping effect, which causes an unstable growing of the estimated system output interval.

[IIII] According to Section 2.1 and the interval observer model (46) related to the application example, α_i satisfies: $0 \leqslant \alpha_i \leqslant 1$ where $i = 1, 2, 3$.

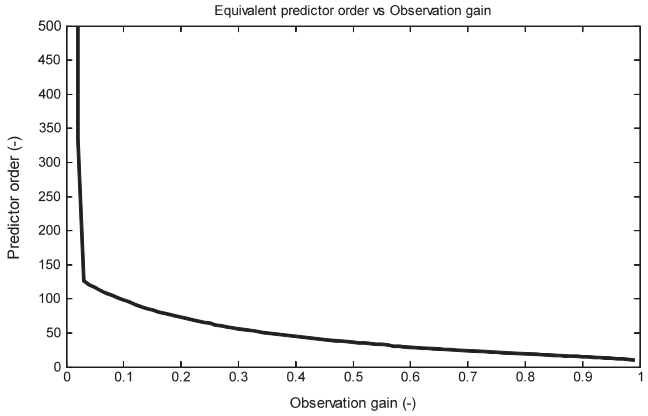

Figure 4. Evolution of the equivalent predictor order regarding the observation gain of its associated interval observer.

4.3. Equivalence between observers and predictors

Using the application example, in this section, the evolution of the equivalent predictor order, λ, regarding the observation gain of its associated interval observer is described. Thus, for a given observer gain, the order λ of the equivalent predictor is obtained using (23) for a certain degree of approximation ε. Then, in Figure 4, the evolution of the predictor order versus the observer gain is plotted considering the parameterization $l_i = \alpha\theta_i$ varying the α from simulation ($\alpha = 0$) to minimum order prediction ($\alpha = 1$) and using an approximation degree given by $\varepsilon = 1e\text{-}5$. It must be taken into account that for a certain value of α, (23) is evaluated considering all the possible trajectories related to the interval observer determined for the uncertainty related to the parameters. It can be noticed that when the observer works as a simulator ($\alpha \to 0$), the order of its equivalent predictor is affected by a fast growing, that is, the memory of the predictor increases fastly. On the other hand, when the observer works as a minimum order predictor ($\alpha \to 1$) (*predictor* of order $n = 3$, being n the system order), the equivalent predictor tends to the order of the system ('dead-beat observer') according to [15]), that is, the memory of the predictor decreases until the system order.

4.4. Time evolution of the residual sensitivity to a fault

In Section 3.3, it was pointed out that the fault residual sensitivity functions of the interval observer and its equivalent $\lambda-$order predictor are equal when the degree of approximation ε can be underestimated because it is roughly zero-valued. Thus, the goal of this section is to exemplify this statement using the application example and considering the residual sensitivity to an output sensor fault, $\boldsymbol{S}_{fy}$, and the residual sensitivity to an input sensor fault, $\boldsymbol{S}_{fu}$.

Such as it was seen in Section 3.3, the functions $\boldsymbol{S}_{fy}$ and $\boldsymbol{S}_{fu}$ are given by (39) and (40), respectively. Concerning these expressions, it must be noticed that they are valid for the interval observer and also for its equivalent predictor. The fault residual sensitivity functions associated with the interval observer are obtained when the functions $\boldsymbol{O}(q^{-1}, \boldsymbol{\theta})$ and $\boldsymbol{V}(q^{-1}, \boldsymbol{\theta})$ are calculated using (27) and (26), respectively. On the other hand, if (29) and (28) were used to calculate those functions, the fault residual sensitivity functions associated with the equivalent predictor would be obtained.

Focusing on the application example, when an interval observer is considered, according to (39) and (47), its residual sensitivity to an output sensor fault is given by

$$\boldsymbol{S}_{ofy}(q^{-1}, \boldsymbol{\theta}) = \boldsymbol{O}_o(q^{-1}, \boldsymbol{\theta})\boldsymbol{G}_{fy}(q^{-1}, \tilde{\boldsymbol{\theta}}) = \frac{1 - \theta_1 q^{-1} - \theta_2 q^{-2} - \theta_3 q^{-3}}{1 + (l_1 - \theta_1)q^{-1} + (l_2 - \theta_2)q^{-2} + (l_3 - \theta_3)q^{-3}} \tag{49}$$

assuming matrix $\boldsymbol{F}_y$ is equal to the identity matrix $\boldsymbol{I}$. Conversely, according to (40) and (47), the interval observer residual sensitivity to an input sensor fault can be written as it follows:

$$\boldsymbol{S}_{ofu}(q^{-1},\boldsymbol{\theta}) = \boldsymbol{V}_o(q^{-1},\boldsymbol{\theta})\boldsymbol{F}_u(\boldsymbol{\theta}) = -\frac{\theta_4 q^{-1}}{1+(k_1-\theta_1)q^{-1}+(k_2-\theta_2)q^{-2}+(k_3-\theta_3)q^{-3}} \quad (50)$$

assuming matrix $\boldsymbol{F}_u = \boldsymbol{I}$.

Concerning the equivalent predictor associated with the interval observer given by (46), its residual sensitivity to an output sensor fault can be obtained using (39), (29), and (20), and considering the matrices $\boldsymbol{A}$ and $\boldsymbol{C}$ associated with the monitored system (45)

$$\begin{aligned}\boldsymbol{S}_{pfy}(q^{-1},\boldsymbol{\theta}) &= \boldsymbol{O}_p(q^{-1},\boldsymbol{\theta})\boldsymbol{G}_{fy}(q^{-1},\tilde{\boldsymbol{\theta}}) = \boldsymbol{I} - \boldsymbol{H}_p(q^{-1},\boldsymbol{\theta}) = (\boldsymbol{I} - \boldsymbol{A}_p(q^{-1},\boldsymbol{\theta})q^{-1}) = \\ &= \boldsymbol{I} - \left(\sum_{v=1}^{\lambda} \boldsymbol{C}(\boldsymbol{\theta})\left(\boldsymbol{A}(\boldsymbol{\theta}) - \boldsymbol{L}\boldsymbol{C}\right)^{v-1}\boldsymbol{L}q^{-(v-1)}\right)q^{-1}\end{aligned} \quad (51)$$

where $\boldsymbol{F}_y = \boldsymbol{I}$, λ is obtained using (23) and $\boldsymbol{L} = [l_3, l_2, l_1]^{\mathrm{t}}$.

Then, using (40), (28), and (21) and the matrices $\boldsymbol{A}$, $\boldsymbol{B}$, $\boldsymbol{C}$, and $\boldsymbol{L}$ associated to the monitored system (45), the equivalent predictor residual sensitivity to an input sensor fault can be calculated computing the following equation

$$\begin{aligned}\boldsymbol{S}_{pfu}(q^{-1},\boldsymbol{\theta}) &= \boldsymbol{V}_p(q^{-1},\boldsymbol{\theta})\boldsymbol{F}_u(\boldsymbol{\theta}) = -\boldsymbol{G}_p(q^{-1},\boldsymbol{\theta}) = -\boldsymbol{B}_p(q^{-1},\boldsymbol{\theta})q^{-1} = \\ &= -\left(\sum_{v=1}^{\lambda} \boldsymbol{C}(\boldsymbol{\theta})\left(\boldsymbol{A}(\boldsymbol{\theta}) - \boldsymbol{L}\boldsymbol{C}\right)^{v-1}\boldsymbol{B}(\boldsymbol{\theta})q^{-(v-1)}\right)q^{-1}\end{aligned} \quad (52)$$

assuming $\boldsymbol{F}_u = \boldsymbol{I}$.

In the following, considering an abrupt fault modeled as a unit-step function, the time evolution of those residual sensitivity functions is plotted using the observer gain set given by $\alpha_1 = \alpha_2 = \alpha_3 = 0.5$ and considering just the nominal value of the uncertain parameters ($\boldsymbol{\theta} = \boldsymbol{\theta}^o \in \boldsymbol{\Theta}$). In this case, the equivalent predictor order is given by $\lambda = 36$ (Figure 4) considering a predictor approximation degree $\varepsilon = 1e\text{-}5$ (23).

In Figure 5, the residual sensitivity functions to an output sensor fault (*upper plot*) and to an input sensor fault (*lower plot*) are drawn using both the nominal observer (*solid line*) and its associated equivalent predictor (*dash line*). As it can be seen from this figure, comparing the time evolution of the residual sensitivity to an input/output fault related to the nominal observer with the one related to the equivalent predictor, they are almost undistinguishable when both approaches are really equivalent.

On the other hand, in Figure 6, the case in which both models are not equivalent is considered. This is achieved considering $\lambda < 36$, for example, $\lambda = 3$. In this case, such as it can be seen in Figure 6, the time evolution of the residual sensitivity to an output/input sensor related to both models is different.

4.5. Predictor and observer behavior in fault scenario

The goal of this section is to compare the fault detection performance of an interval observer whose system output estimations are obtained using the *trajectory-based approach* [21] with the fault detection performance of its corresponding equivalent predictor considering the fault scenario used in Section 4.2 and assuming a predictor approximation degree $\varepsilon = 1e\text{-}5$ (23). In addition, this performance comparison is also used to confirm that the equivalent predictor also avoids the wrapping effect such as the interval observer when it is computed using the *trajectory-based approach* [24].

A case where both type of models are fully equivalent regarding fault detection is shown in Figure 7. This is achieved when the order of the equivalent predictor λ is equal to 36 (23), and the observer gains mentioned in Section 4.2 are used ($\alpha_1 = \alpha_2 = \alpha_3 = 0.5$). Then, in Figure 7, the

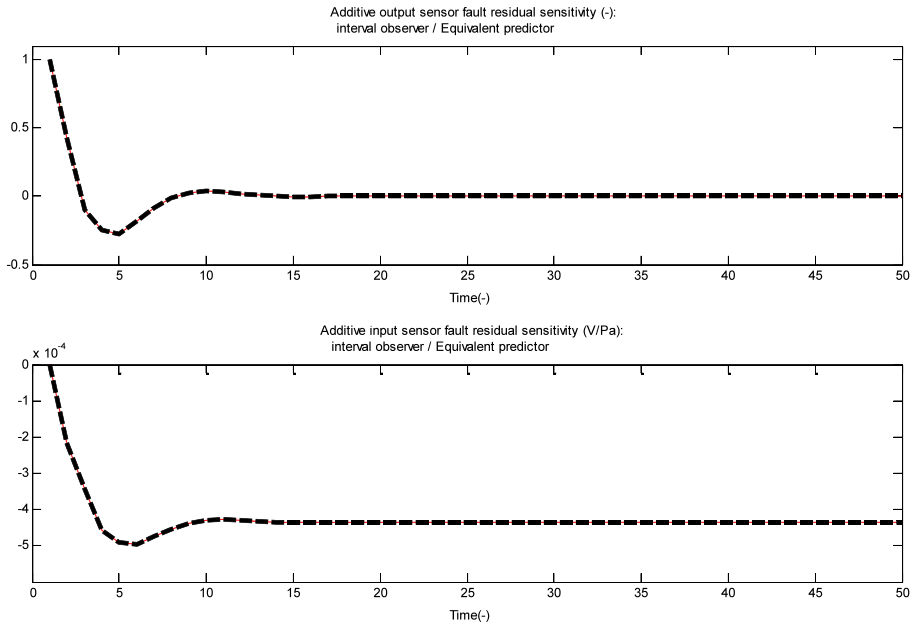

Figure 5. Time evolution of the residual sensitivity function to an output sensor fault (*upper plot*) and the residual sensitivity function to an input sensor fault (*lower plot*) using the nominal observer (*solid line*) and its equivalent predictor (*dash line*). [Colour figure can be viewed at wileyonlinelibrary.com]

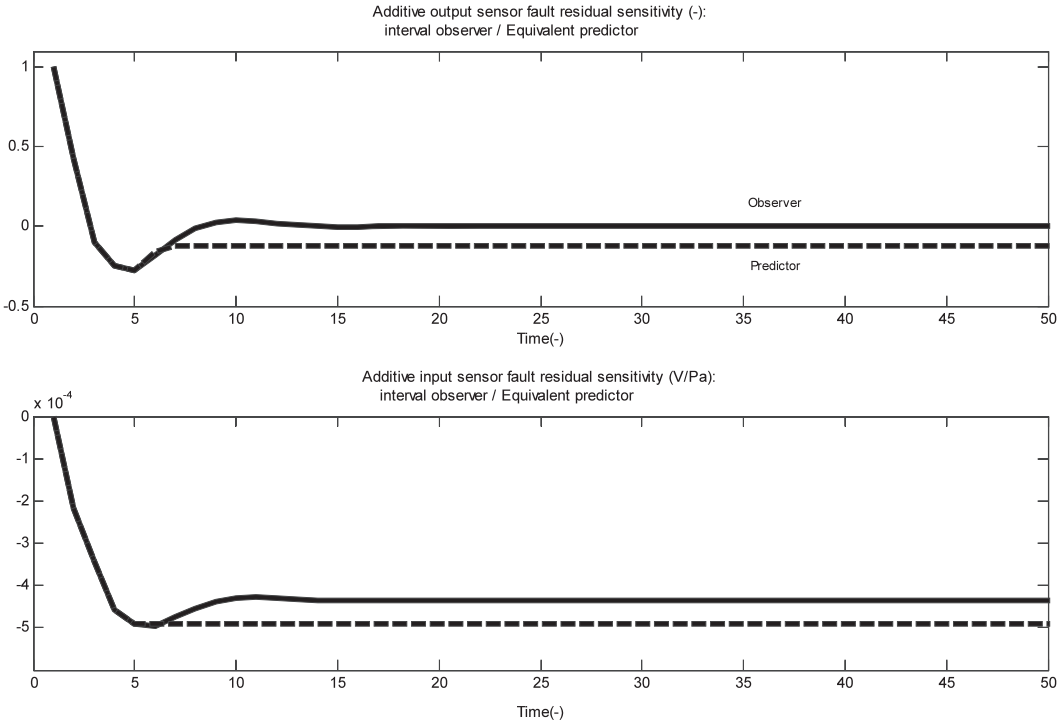

Figure 6. Time evolution of the residual sensitivity function to an output sensor fault (*upper plot*) and the residual sensitivity function to an input sensor fault (*lower plot*) using the nominal observer (*solid line*) and its equivalent predictor (*dash line*), which does not satisfy condition (23).

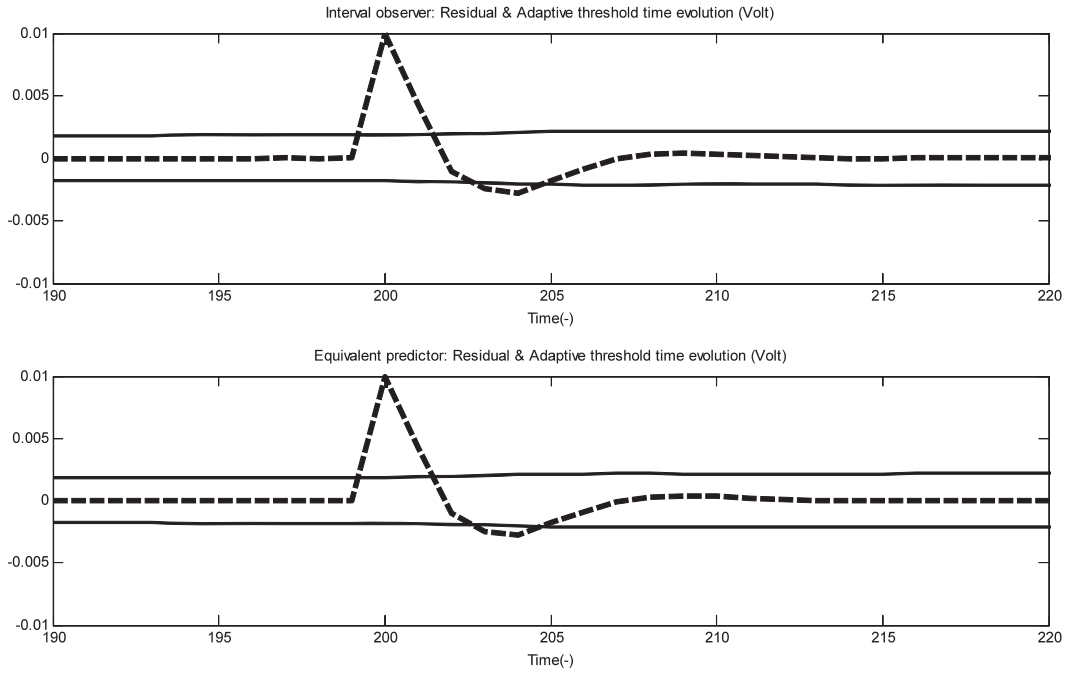

Figure 7. Time evolution of the nominal residual (*dash line*) and its adaptive threshold (*solid line*) using the interval observer (*upper plot*) and its equivalent predictor (*lower plot*) using $\lambda = 36$.

time evolutions of the nominal residual (*green line*) ((47), $\boldsymbol{\theta} = \boldsymbol{\theta}^o \in \boldsymbol{\Theta}$) and its associated adaptive threshold (*blue line*) (33) are plotted between the time instants *190* and *220* using both models (*interval observer: upper plot*; *equivalent predictor: lower plot*) showing the full equivalence between them. As a result, the interval observer and its correspondent predictor are also equivalent regarding their fault detection properties according to the fault detection test given by (35).

4.6. Computing the equivalent predictor interval output using two known point-wise trajectories

As discussed in Section 2.5, when the observation gain condition given by (48) ($l_3 = 1$) is forced, the observer output interval can be computed using the *set-based approach* avoiding the wrapping effect [24]. That is because the interval observer matrix ($\boldsymbol{A_o} = \mathbf{A\text{-}LC}$) fulfils the positive property (all its elements are positive) and thus, according to [25, 27]), the trajectory of the output interval upper bound is obtained when the uncertain parameters are equal to their interval upper bound ($\bar{\hat{y}}(k) = \hat{y}(k, \bar{\theta}_1, \bar{\theta}_2, \bar{\theta}_3, \bar{\theta}_4)$) while the trajectory of the output interval lower bound is obtained when the parameters are equal to their interval lower bound ($\underline{\hat{y}}(k) = \hat{y}(k, \underline{\theta}_1, \underline{\theta}_2, \underline{\theta}_3, \underline{\theta}_4)$). Conversely, these two system output interval trajectories could also be generated by the equivalent predictor using the uncertain parameter lower and upper bounds what means that the output interval can be also generated by the equivalent predictor using only two known point-wise trajectories, and consequently, its computational cost is lower than that corresponding to the general *trajectory-based approach*.

In the following, the next observation gains are considered: $\alpha_1 = \alpha_2 = 0.5$ and $\alpha_3 = 1$. Then, assuming an equivalent predictor approximation degree $\varepsilon = 1e\text{-}5$, the equivalent predictor order is given by $\lambda = 112$. Considering those observer and predictor parameters, the system output estimation interval (*solid line*) and its nominal value are generated (*dot line*) in Figure 8 using the interval observer computed by the *set-based approach* (*upper plot*) and its equivalent predictor computed using only the two known point-wise trajectories (*lower plot*) such as it was mentioned before. Besides, the time evolution of the system output measurement is also plotted (*dash line*). Figure 8 shows how both methods generate exactly the same interval output, and consequently, they are equivalent regarding their fault detection performance.

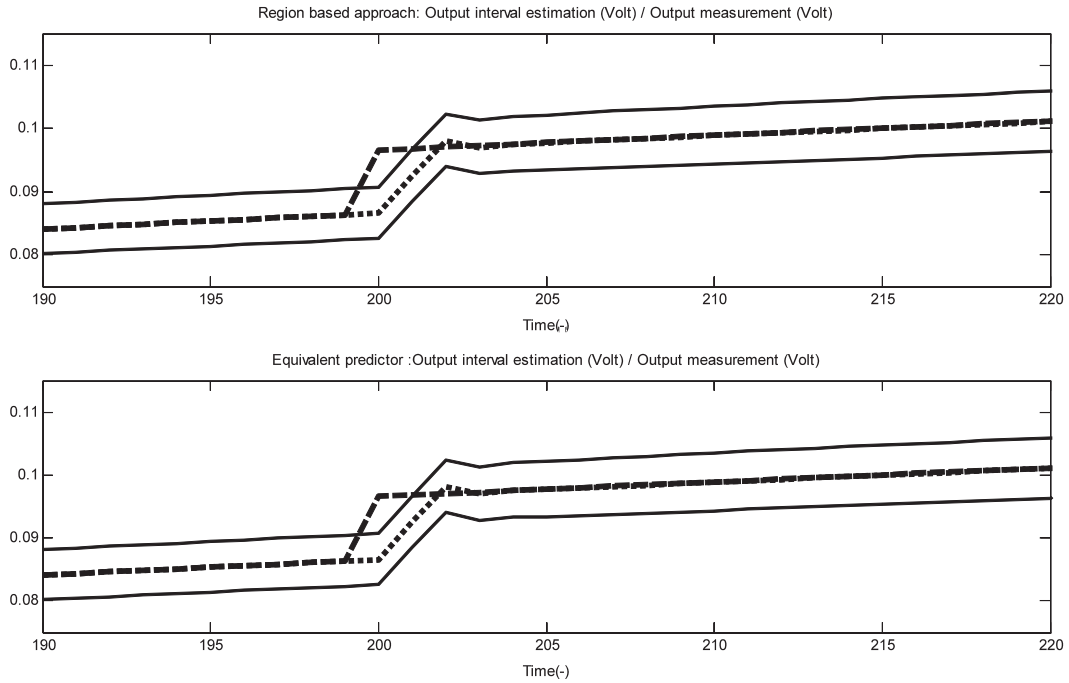

Figure 8. Time evolution of the system output estimation interval (solid line) and its nominal value (*dot line*), and the output sensor measurement (*dash line*) using the interval observer (*upper plot*) and its equivalent predictor (*lower plot*).

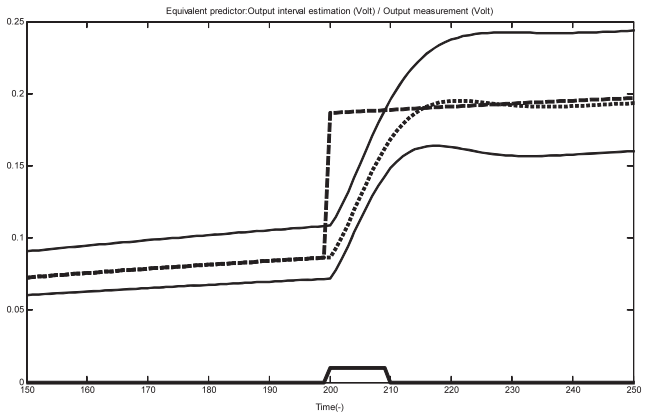

Figure 9. Time evolution of the system output estimation interval (*solid line*) and its nominal value (*dot line*), and the output sensor measurement (*dash line*) using a $\lambda-$order predictor ($\lambda = 117$). The fault indicator is plotted below in *solid line*.

4.7. Influence of the predictor order λ on the fault indication persistence

Finally, the discussion presented in Section 3.3 and Table I about the effect of the predictor order λ on the fault indication persistence will be illustrated. Meseguer *et al.* [13] show that when interval observers are used, the observer gain has an important influence on the fault indication persistence. In general, the fault indication persistence depends on the observer gain, on the dynamics of the fault residual sensitivity, and on the parameter uncertainty. Moreover, as indicated in Meseguer *et al.* [13], when the simulation approach can not detect the fault and the '*dead-beat observer*' [15] can only detect during a number of time instants equal to its order, optimum observer gain values between *simulation* and *minimum order prediction* can be used in order to enhance the fault indication persistence. When instead of using the interval observer, its equivalent $\lambda-$order predictor

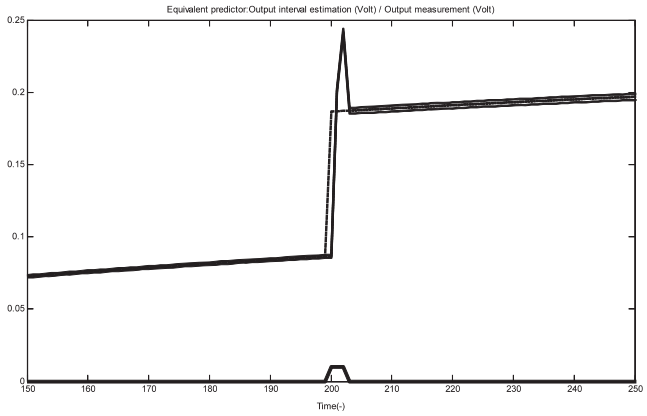

Figure 10. Time evolution of the system output estimation interval (solid line) and its nominal value (*dot line*), and the output sensor measurement (*dash line*) using a $\lambda-$order predictor (λ *=3*). The fault indicator is plotted below in *solid line*.

is used; the order λ of this model plays the same role regarding the fault indication persistence than the observer gain, derived from the shown equivalence between both models (Figure 4).

Next, assuming a constant additive fault affecting the system output sensor occurring at time instant t_0 =200 and whose value is given by f *=0.1 Volt* (roughly, *1 time* of the steady-state system output nominal value), the time evolution of the system output estimation interval (solid line) and its nominal value (*dot line*) generated by the equivalent predictor are plotted. In addition, the time evolution of the system output measurement (*dash line*) and the fault detection indicator (*solid line*) are also plotted. In Figure 9, a predictor whose order is λ *=117* is considered. This is equivalent to the observer given by (46) when $\alpha_1 = \alpha_2 = \alpha_3$ *=0.05* ($l_i = \alpha_i \theta_i$) and ε *=1e-5* (see Figure 4 in Section 4.3). On the other hand, in Figure 10, the predictor of minimum order is used (λ *=3*), which is equivalent to the interval observer when $\alpha_1 = \alpha_2 = \alpha_3$ *=1* and ε *=1e-5.*

5. CONCLUSIONS

This paper demonstrates that it is possible to determine a $\lambda-$order interval predictor, which is fully equivalent to an interval observer for a given observer gain $\boldsymbol{L}$ when applied to fault detection applications. The presented method is an extension of the approach presented by Chow and Wilsky [5] where the predictor of minimum order ('*dead-beat observer*' [15]) was obtained. In the presented approach, the order of the equivalent predictor is determined by the observer gain matrix $\boldsymbol{L}$ and offers to the predictor model the same fault indication persistence than the corresponding to the interval observer. Such equivalence is based on the fact that an interval observer can be represented by an ARMA model, while a predictor by an MA model, and it is known from the literature that an ARMA model can be approximated by an MA model of infinite order. On the other hand, this paper points out that the use of the $\lambda-$order equivalent predictor is very interesting in fault detection applications because it avoids those problems associated with the state estimation as the initial state value problem or the wrapping effect. In addition, the equivalent predictor can be computed efficiently if the associated interval observer fulfils the positive property, which can be forced using the observer gains [24]. In this case, the interval output generated by the equivalent predictor is determined by two known point-wise trajectories obtained when the uncertain parameters are equal to their interval upper and lower bounds [25].

As a future work, the results presented in this paper could be extended to deal with fault distinguihsability and multiple faults. The inclusion of other sources of uncertainty as noise and disturbances in an unknown but bounded context should also be considered.

APPENDIX: PROOF OF PROPOSITION 1

Given a $\boldsymbol{\theta} \in \boldsymbol{\Theta}$, the observer matrix can be decomposed as follows

$$\boldsymbol{A}_o(\boldsymbol{\theta}) = \boldsymbol{T}(\boldsymbol{\theta})\boldsymbol{\Lambda}_o(\boldsymbol{\theta})\boldsymbol{T}^{-1}(\boldsymbol{\theta}) \tag{A.1}$$

where $\boldsymbol{\Lambda}_o(\boldsymbol{\theta})$ is a diagonal matrix. Then,

$$\left\| \boldsymbol{A}_o(\boldsymbol{\theta})^k \right\|_\infty = \left\| (\boldsymbol{T}(\boldsymbol{\theta})\boldsymbol{\Lambda}_o(\boldsymbol{\theta})\boldsymbol{T}^{-1}(\boldsymbol{\theta}))^k \right\|_\infty \leqslant \|\boldsymbol{T}(\boldsymbol{\theta})\|_\infty \left\| \boldsymbol{T}^{-1}(\boldsymbol{\theta}) \right\|_\infty \rho(\boldsymbol{A}_o(\boldsymbol{\theta}))^k = \kappa(\boldsymbol{\theta})\rho(\boldsymbol{A}_o(\boldsymbol{\theta}))^k \tag{A.2}$$

where ρ is the spectral radius of the interval observer matrix $\boldsymbol{A}_o$ determined by the maximum absolute value of all the eigenvalues of this matrix and κ is the condition number of $\boldsymbol{A}_o$.

In order to determine the value λ_ε such that $\left\| \boldsymbol{A}_o(\boldsymbol{\theta})^k \right\|_\infty \leqslant \varepsilon$ for $k \geqslant \lambda_\varepsilon$ with $0 \leqslant \varepsilon < 1$, we impose

$$\kappa(\boldsymbol{\theta})\rho(\boldsymbol{A}_o(\boldsymbol{\theta}))^{\lambda_\varepsilon} \leqslant \varepsilon \tag{A.3}$$

Taking logarithms

$$log\kappa(\boldsymbol{\theta}) + \lambda_\varepsilon log\, \rho(\boldsymbol{A}_o(\boldsymbol{\theta})) \leqslant log\varepsilon \tag{A.4}$$

Notice that because $0 \leqslant \varepsilon < 1$ and the observer is designed to be stable (i.e., $\rho(\boldsymbol{A}_o(\boldsymbol{\theta})) < 1$), some of the previous logarithms will be negative. Thus, A.4 can be reformulated as follows

$$log\kappa(\boldsymbol{\theta}) - \lambda_\varepsilon \, |log\rho(\boldsymbol{A}_o(\boldsymbol{\theta}))| \leqslant -|log\varepsilon| \tag{A.5}$$

and the value of λ_ε can be determined as follows

$$\lambda_\varepsilon \geqslant \frac{|log\varepsilon| + log\kappa(\boldsymbol{\theta})}{|log\rho(\boldsymbol{A}_o(\boldsymbol{\theta}))|} \tag{A.6}$$

Finally, considering that λ_ε should work for all $\boldsymbol{\theta} \in \boldsymbol{\Theta}$,

$$\lambda_\varepsilon \geqslant \max_{\boldsymbol{\theta} \in \boldsymbol{\Theta}} \frac{|log\varepsilon| + log\kappa(\boldsymbol{\theta})}{|log\rho(\boldsymbol{A}_o(\boldsymbol{\theta}))|} \tag{A.7}$$

The computation of λ_ε using (A.7) can be performed in an approximate way by gridding or in a more elaborate way using the bisection algorithm presented in Puig *et al.* [21].

Remark

This proof relies on the procedures to bound the norm of the power of matrix proposed in Higham [31]. However, as discussed in Higham [31], the bound (A.2) could be unsatisfactory when the matrix have well-conditioned large eigenvalues and ill-conditioned small eingenvalues. And, moreover, because it assumes the norm of matrix power is non-monotonically decreasing when it could present large humps. Higham [31] proposes other methods more ellaborated for computing this bound that could be used to improve the previous proof from the numerical point of view.

ACKNOWLEDGEMENTS

This work has been partially funded by the Spanish Government (MINECO) through the project CICYT ECOCIS (ref. DPI2013-48243-C2-1-R) and by MINECO and FEDER through the project CICYT HARCRICS (ref. DPI2014-58104-R).

REFERENCES

1. Blanke M, Kinnaert M, Lunze J, Staroswiecki M, Schröder J. *Diagnosis and Fault-Tolerant Control*. Springer-Verlag: New York, 2006.
2. Chen J, Patton RJ. *Robust Model-Based Fault Diagnosis for Dynamic Systems*. Kluwer Academic Publishers: Boston, 1999.
3. Gertler JJ. *Fault Detection and Diagnosis in Engineering Systems*. Marcel Dekker: New York, 1998.
4. Isermann R. *Fault-diagnosis systems: an introduction from fault detection to fault tolerance*. Springer: Berlin, 2006.
5. Chow EY, Willsky AS. Analytical redundancy and the design of robust detection systems. *IEEE Transactions on Automatic Control* 1984; **29**(7):603–614.
6. Ploix S, Adrot O. Parity relations for linear uncertain dynamic systems. *Automatica* 2006; **42**(9):1553–1562.
7. Puig V, Quevedo J, Escobet T, De las Heras S. Passive robust fault detection of dynamic processes using interval models. *IEEE Transactions on Control Systems Technology* 2008; **16**(5):1083–1089.
8. Sainz MA, Armengol J, Vehí J. Fault detection and isolation of the three-tank system using modal interval analysis. *Journal of Process Control* 2002; **12**(2):328–338.
9. Montes de Oca S, Puig V, Blesa J. Robust fault detection based on adaptive threshold generation using interval LPV observers. *International Journal of Adaptive Control and Signal Processing* 2012; **26**(3):258–283.
10. Puig V, Stancu A, Escobet T, Nejjari F, Quevedo J, Patton RJ. Passive robust fault detection using interval observers: application to the DAMADICS benchmark problem. *Control Engineering Practice* 2006; **14**(6):621–633.
11. Raïssi T, Videau G, Zolghadri A. Interval observer design for consistency checks of nonlinear continuous-time systems. *Automatica* 2010; **46**(3):518–527.
12. Puig V, Blesa J, Saludes J, Fernández-Cantí JM. Set-membership parity space approach for fault detection in linear uncertain dynamic systems. *International Journal of Adaptive Control and Signal Processing* 2014. Article first published online. DOI: 10.1002/acs.2476.
13. Meseguer J, Puig V, Escobet T. Observer gain effect in linear interval observer-based fault detection. *Journal of Process Control* 2010a; **20**(8):944–956.
14. Ding SX. *Model-based Fault Diagnosis Techniques Design Schemes, Algorithms, and Tools*. Springer: Berlin, 2008.
15. Patton RJ, Chen J. A review of parity space approaches to fault diagnosis. *Proc. IFAC Symp. Fault Detection, Supervision and Safety for Thecnical Processes, SAFEPROCESS*, Vol. 1, Baden-Baden, Germany, 1991; 65–81, pp. 239-255.
16. Kühn W. *Rigorously computed orbits of dynamical systems without the wrapping effect*, 1998. Computing 61, 47-67. 1998.
17. Puig V, Stancu A, Quevedo J. Set versus trajectory based approaches to interval observation. *Conference on Decision and Control & European Control Conference (CDC-ECC'05)*, Sevilla. Spain, 2005a; 6567–6572.
18. Blesa J, Puig V, Saludes J. Identification for passive robust fault detection using zonotope-based set-membership approaches. *International Journal of Adaptive Control and Signal Processing* 2011; **25**(9):788–812.
19. Jacques P, Hamelin F, Aubrun C. Optimal fault detection in a closed-loop framework: a joint approach. *IFAC SAFEPROCESS '03*, Washington DC. USA, 2003; 105-111.
20. Chilali M, Gahinet P, Apkarian P. Robust Pole Placement in LMI Regions. *IEEE Trans. Automatic Control* 1996; **41**(3):436–442.
21. Puig V, Saludes J, Quevedo J. Worst-case simulation of discrete linear time-invariant interval dynamic systems. *Reliable Computing* 2003; **9**(4):251–290.
22. Meseguer J, Puig V, Escobet T. Fault diagnosis using a timed discrete-event approach based on interval observers: application to sewer networks. *IEEE Transactions on Systems Man and Cybernetics Part A-Systems and Humans* 2010b:40 - 5,pp. 900 - 916, 09/2010.
23. Kailath T. *Linear Systems*. Prentice-Hall: NY, USA, 1980.
24. Meseguer J, Puig V, Escobet T. Robust fault detection linear interval observers avoiding the wrapping effect. *IFAC World Congress 2008*, Seul, Korea, 2008; 11570–11575.
25. Cugueró P, Puig V, Saludes J, Escobet T. A class of uncertain linear interval models for which a set based robust simulation can be reduced to few pointwise simulations. *In Proceedings of Conference on Decision and Control 2002 (CDC'02)*, Las Vegas. USA, 2002; 1862–1863.
26. Efimov D, Perruquetti W, Raïssi T, Zolghadri A. On interval observer design for time-invariant discrete-time systems. *European Control Conference, (ECC'2013)*, Zurich, Switzerland, 2013; 2651–2656.
27. Mazenc F, Dinh TN, Niculescu SI. Interval observers for discrete-time systems. *International Journal of Robust and Nonlinear Control* 2013; **24**(17):2867–2890.
28. Puig V, Schmid F, Quevedo J, Pulido B. A new fault diagnosis algorithm that improves the integration of fault detection and isolation. *Conference on Decision and Control & European Control Conference (CDC-ECC'05)*, Sevilla. Spain, 2005b; 3809–3814.
29. Bartys M, Patton R, Syfert M, de las Heras S, Quevedo J. Introduction to the DAMADICS actuator FDI benchmark study. *Control Engineering Practice* 2006; **14**(6):577–596.
30. Ploix S, Adrot O, Ragot J. Parameter uncertainty computation in static linear models. *38*th *IEEE Conference on Decision and Control*, Vol. 2, Phoenix, Arizona, USA, 1999; 1916–1921.
31. Higham NJ. *Accuracy and Stability of Numerical Algorithms* (Second Edition), Society for Industrial and Applied Mathematics. Philadelphia, USA, 2002.